JOURNAL OF MATERIALS SCIENCE 15 (1980) 2335–2344

The sinterability of ultrafine WC powders obtained by a CVD method

JUNICHI HOJO, RYOICHI OONO, AKIO KATO
Department of Applied Chemistry, Faculty of Engineering, Kyushu University, Fukuoka, 812, Japan

The sintering behaviour of ultrafine WC powders produced by a CVD method (particle size $< 0.3\,\mu m$) and commercial WC powders (particle size $\sim 1\,\mu m$) is investigated in hydrogen and in vacuum. It has been found that ultrafine WC powders have an extremely high sinterability and give a sintered body with a relative density of 100% by sintering at a considerably lower temperature than normal, such as 1750° C. Also WC powders with a large particle size and a wide-size distribution have a high sinterability caused by the presence of fine particles and the sinterability of WC powders is influenced significantly by the sintering atmosphere. The atmospheric effect is discussed in connection with the heating behaviour of a surface oxide layer and free carbon.

1. Introduction

The carbides of transition elements in Groups IV, V and VI of the periodic table are referred to as "refractory carbides" and have extremely high melting points, hardness and good corrosion resistance. In recent years, the interest in the carbides has increased because of their excellent applicabilities to superhigh temperature techniques as compared to refractory metals and oxide ceramics. However, their low sinterabilities are a serious disadvantage. The use of fine powders is expected to be most useful for the improvement of sinterabilities of refractory materials.

The authors have reported the formation of ultrafine powders of tungsten carbide (WC) by a CVD method [1]. WC is a most important carbide as the major constituent in superhard alloys. In the present work, the sintering behaviour of the ultrafine WC powders was investigated in hydrogen and in vacuum.

2. Experimental details

2.1. Materials

Three kinds of WC powders with different particle sizes and compositions were produced by the vapour phase reaction of the WCl_6–CH_4–H_2 system (1400° C) (abbreviated as A–WC, B–WC and D–WC). Commercial WC powders were also used (Mitsuwa's Pure Chemicals, abbreviated as C–WC).

2.2. Sintering

Carbide powders, mixed with glycerine (1 to 2 wt %)* as plasticizer, were pressed at 450 MN m^{-2} by use of a single action steel die. The pellet size was 10 mm in diameter and about 0.5 mm thick. A graphite box was used as the container for the pellet. In the sintering in hydrogen, a recrystallized alumina tube (internal diameter 22 mm) and a SiC resistance furnace were used for heating. The hydrogen was deoxygenated with activated copper and dried with a silica gel column and a liquid nitrogen trap, the flow rate of which was 100 ml min^{-1}. The sintering was started by moving the sample from the low temperature zone (900° C) to the centre of the furnace after the furnace was heated up to a given temperature. In the sintering in vacuum, a high frequency induction furnace with a molybdenum susceptor was used for heating. The reactor was evacuated to a pressure

---

*It was confirmed by a thermogravimetric analysis that the glycerine in the compact vaporized completely by heating at 10° C min^{-1} up to about 400° C in hydrogen. In the sintering in vacuum, the compact was pre-heated up to 500° C in hydrogen to remove the glycerine.

below 10^{-3} mm Hg using an oil diffusion pump. The heating rate was about 100° C min^{-1} over the temperature range extending from 900° C to a given temperature in both hydrogen and vacuum.

2.3. Characterization of powders and sintered bodies

The particle size of the powders was determined by transmission electron microscope (TEM) observation. The specific surface area was measured by single point-BET method. The free carbon content was determined by a combustion analysis of the carbon residue after the treatment of samples with an HF–HNO_3 mixture. The oxygen content was determined by thermogravimetric analysis of CO evolved by heating at 700 to 1100° C in helium. The impurity metals were identified by emission spectrochemical analysis.

The linear shrinkage of the compact was determined by measuring the diameter with a cathetometer. The relative density to the X-ray density of WC (15.8 g cm^{-3} [2]) was calculated from the porosity of open pores determined by weighing the pellet vacuum-impregnated with water and porosity of closed pores determined by weighing this impregnated pellet in water (error ± 1%). The phases contained in the sintered bodies were identified by X-ray diffractometry (Co$K\alpha$ line). The microstructure was observed with a scanning electron microscope (SEM). The micro-hardness was measured with Vickers micro-hardness tester (error ± 100 kg mm^{-2}).

3. Results

3.1. Properties of the original powders

Electron micrographs of the original powders used are shown in Fig. 1 and their properties are summarized in Table I. WC powders produced by the CVD method (A, B and D–WC) consist of nearly spherical particles with a narrow size distribution. The weighted mean diameter of B–WC is the largest among the CVD-powders. Commercial WC powders (C–WC) consist of large particles with irregular shapes. Although the weighted mean diameter of the C–WC is as large as 1 μm, C–WC has a wide size distribution and contains a con-

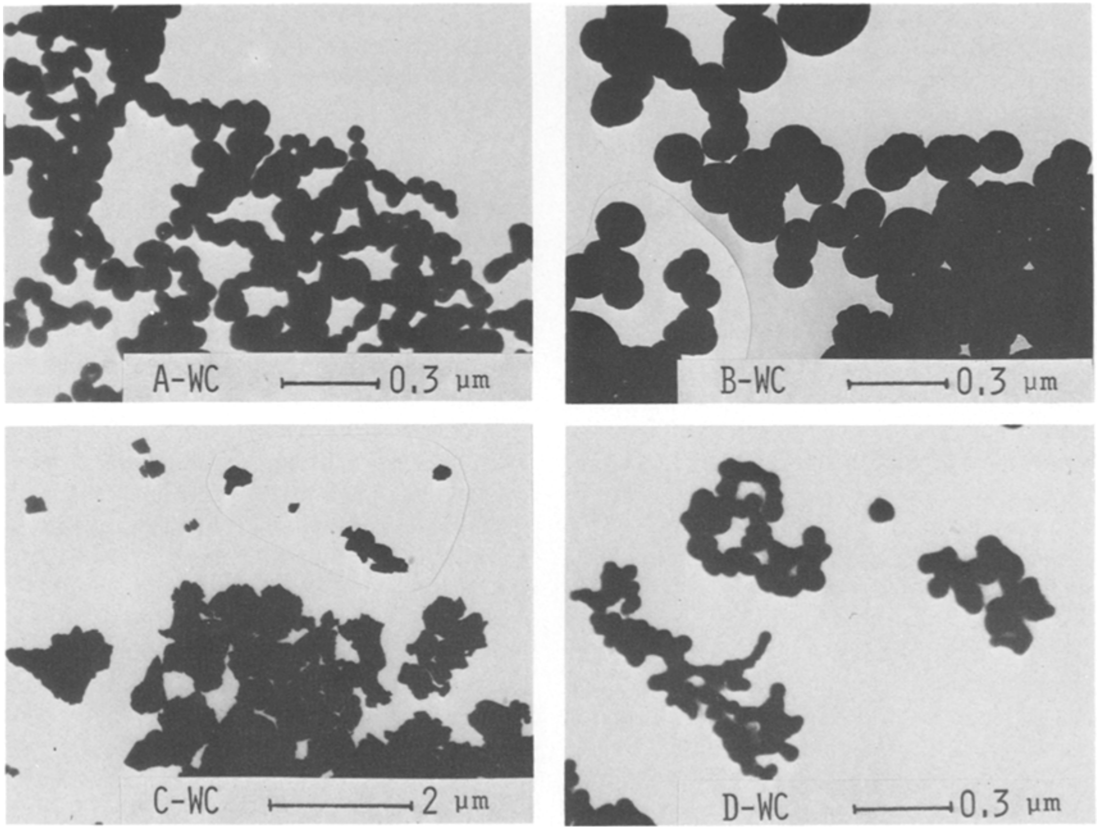

Figure 1 TEM photographs of WC powders.

TABLE I Properties of WC powders

Sample	Specific surface area ($m^2 g^{-1}$)	Weight mean diameter (μm)	Chemical composition (wt%)*			Bulk density of compact (%)
			Total C	Free C	O	
A–WC	4.9	0.06	6.4	0.5	0.3	38–43
B–WC	3.1	0.23	6.7	0.9	0.3	32–35
C–WC	1.7	1.0	6.18†	0.03†	0.4	48–52
D–WC	4.2	0.07	5.9	0.9‡	1.9	41–44

*Based on dry powders. †Given by the maker.

‡For D–WC, which contained 9 wt% W_2C and 4 wt% W by X-ray analysis, the free carbon content was calculated from the phase and chemical compositions.

siderable number of fine particles with the size below 0.3 μm.

The free carbon contents of WC powders produced by the CVD method are larger than those of commercial WC powders. All samples contain oxygen as an impurity which may form an oxide layer at the surface of particles. In particular sample D–WC contains a lot of oxygen. D–WC has a total carbon content less than that required by the stoichiometry of WC and contains small amounts of W_2C and W. The results of emission spectrochemical analysis are summarized in Table II.

3.2. Sintering in hydrogen

3.2.1. Density of sintered body

The variations of linear shrinkage and relative density of WC sintered for 0.5 h in hydrogen with sintering temperature are shown in Fig. 2. The densities of the sintered bodies obtained from WC powders produced by the CVD method increase remarkably above 1300° C. Among the CVD-powders, A–WC and D–WC give sintered bodies with higher densities than those for B–WC. In the sintering of commercial WC powders, the increase in density of the sintered body with temperature is small even at 1500° C, although C–WC has a higher bulk density of compact and give sintered bodies with a higher density at lower temperatures than A, B and D–WC do.

TABLE II Emission spectrochemical analysis of WC powders*

Sample	Al	Si	Ca	Mg	Mo	Cu	Fe	Co	Ti
A–WC	a	a	b	b	b	c	c		
B–WC	a	a	b	b	b	c			
C–WC		a	c		b	c	c	b	b
D–WC	a	a	b	b	b	c	c		

*The orders of impurity-metal contents estimated from the intensities of spectrum lines on films are: a, 100 to 1000 ppm; b, 10 to 100 ppm; c, 1 to 10 ppm.

The variations of linear shrinkage and relative density of WC sintered at 1500° C in hydrogen with sintering time are shown in Fig. 3. In all cases, the linear shrinkages increase remarkably during the heating process up to 1500° C, indicating that the densification of the compact occurs rapidly to a considerable extent at an early stage of sintering.

3.2.2. Microstructure

The fracture surfaces of sintered bodies were observed using SEM. A remarkable grain growth was observed in the sintering of all the WC powders as the sintering temperature was raised from 1300° C to 1500° C. Fig. 4 shows the microstructures of A, B and C–WC sintered at

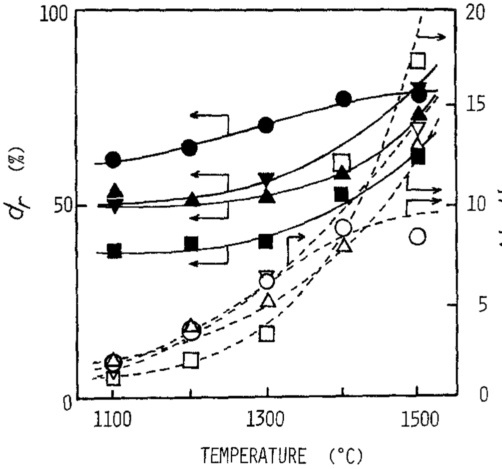

Figure 2 Effects of temperature on the sintering of WC powders in hydrogen (heating: 0.5 h). – – – –, Linear shrinkage ($\Delta L/L_0$). ———, Relative density (d_r). △, ▲: A–WC; □, ■: B–WC; ○, ●: C–WC: ▽, ▼: D–WC.

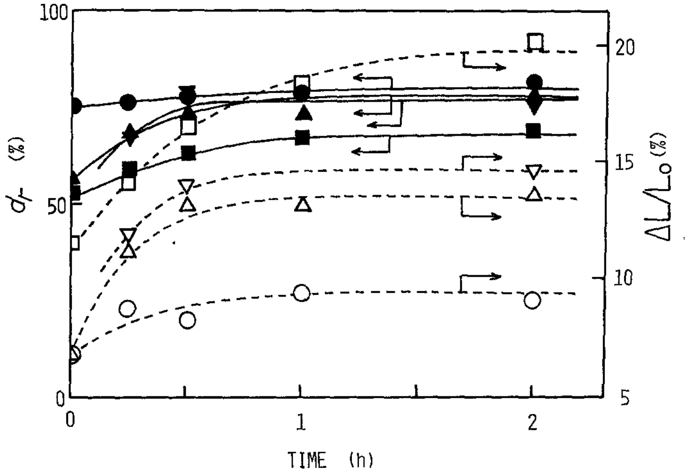

Figure 3 Sintering of WC powders at 1500° C in hydrogen. The symbols are the same as in Fig. 2.

1500° C in hydrogen. The grain growth in the samples from A and B–WC becomes observable after a sintering time of 0.5 h. After 2 h sintering, the grain size of A–WC is about 0.6 μm while that of B–WC is about 0.3 μm. In the sintered body of C–WC with a wide-size distribution, fine particles with a size below 1 μm disappear and grains grow to between 1 and 3 μm. Fig. 5 shows the microstructures of D–WC sintered at 1500° C in hydrogen. The grain growth is unusually vigorous. The sintered D–WC consists of grains with a size of 1 to 4 μm and well-developed facets, although there are some extremely large grains which are greater than 10 μm.

3.3. Sintering in vacuum

3.3.1. Density of sintered body

The linear shrinkage and relative density of WC sintered for 0.5 h in vacuum are shown against sintering temperature in Fig. 6. The densities of the sintered A and B–WC increase more markedly with rise in temperature in vacuum than in hydrogen and become 100% at 1750° C. On the other hand, the increment of the density of the sintered C–WC is slight up to 1750° C and becomes rapid above 1800° C. For sample D–WC, the density is appreciably smaller than those of A and B–WC, although the fineness of the original powders is similar between D and A–WC.

3.3.2. Microstructure

Fig. 7 shows the microstructures of A and B–WC sintered at 1500° C and 1750° C in vacuum. Both A and B–WC sintered at 1500° C in vacuum have similar grain sizes to those obtained at the same temperature in hydrogen. At 1750° C, remarkable grain growth occurs in both sintered bodies, where the sintered A–WC consists mainly of grains with a size of 0.5 to 1.5 μm and the sintered B–WC has a uniform microstructure with a grain size of about 2 μm.

Fig. 8 shows the microstructures of C and D–WC sintered at 1500° C and 1800° C in vacuum. The sintered C–WC contains a great number of fine particles with a size below 1 μm even at 1800° C. The sintered D–WC consists of irregular-shaped grains with a size of about 0.5 μm at 1500° C and with a size of about 1 μm at 1800° C. These grain sizes are smaller than those of the same sample sintered in hydrogen. In the sintering of C and D–WC in vacuum, both the grain growth and densification are retarded relative to the sintering of their samples in hydrogen.

3.4. Foreign phases appearing in WC sintering

Phases other than the WC phase were identified by X-ray diffraction of the pellet surface. The foreign phases detected are listed in Table III. In the A–WC sinter, no foreign phases are detected at any temperature either in hydrogen or in vacuum. In the B–WC sinter, metallic tungsten appears at 1100° C in vacuum. In the C–WC sinter, metallic tungsten appears at 1100° C in hydrogen, while in vacuum the appearing foreign phase changes from W to W_2C with the rise in temperature. In the D–WC sinter, metallic tungsten is detected at 1100° C in hydrogen.

3.5. Hardness of sintered WC

The relationship between micro-hardness and relative density of sintered WC is shown in Fig. 9.

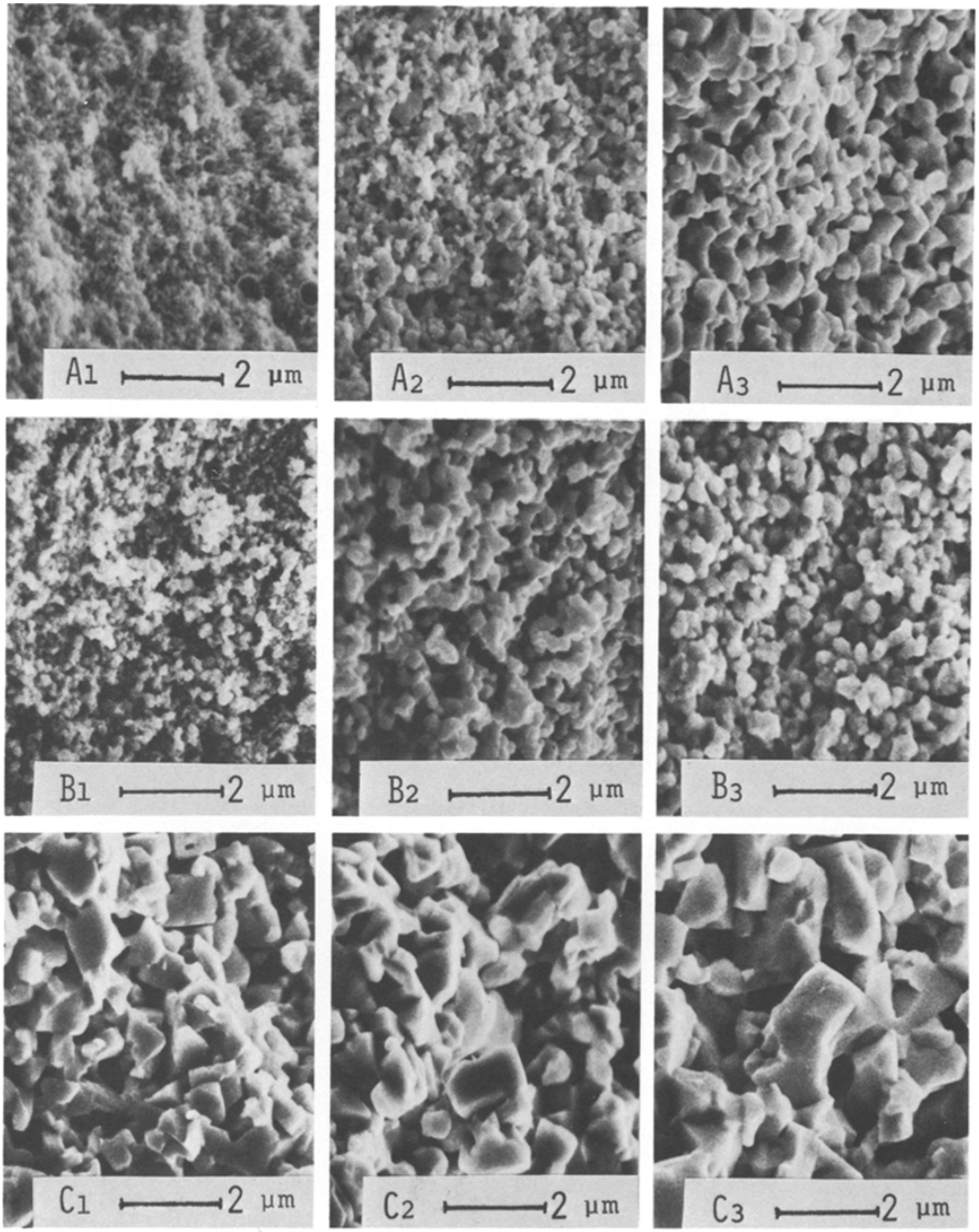

Figure 4 SEM photographs of fracture surfaces of A–WC, B–WC and C–WC sintered at 1500° C in hydrogen. Sample (sintering time) – A_1: A–WC (0 h); A_2: A–WC (0.5 h); A_3: A–WC (2 h); B_1: B–WC (0 h); B_2: B–WC (0.5 h); B_3: B–WC (2 h); C_1: C–WC (0 h); C_2: C–WC (0.5 h); C_3: C–WC (2 h).

Regardless of the differences in the original powders and atmospheres, the hardness of the sintered body increases linearly with increase in the relative density and becomes about 1500 kg mm^{-2} at the relative density of 100%. The SEM photograph shown in Fig. 9 is the etched section of the B–WC sintered to the density of 100% (etchant: 10% $K_3[Fe(CN)_6]$ –10% KOH aqueous solution), where

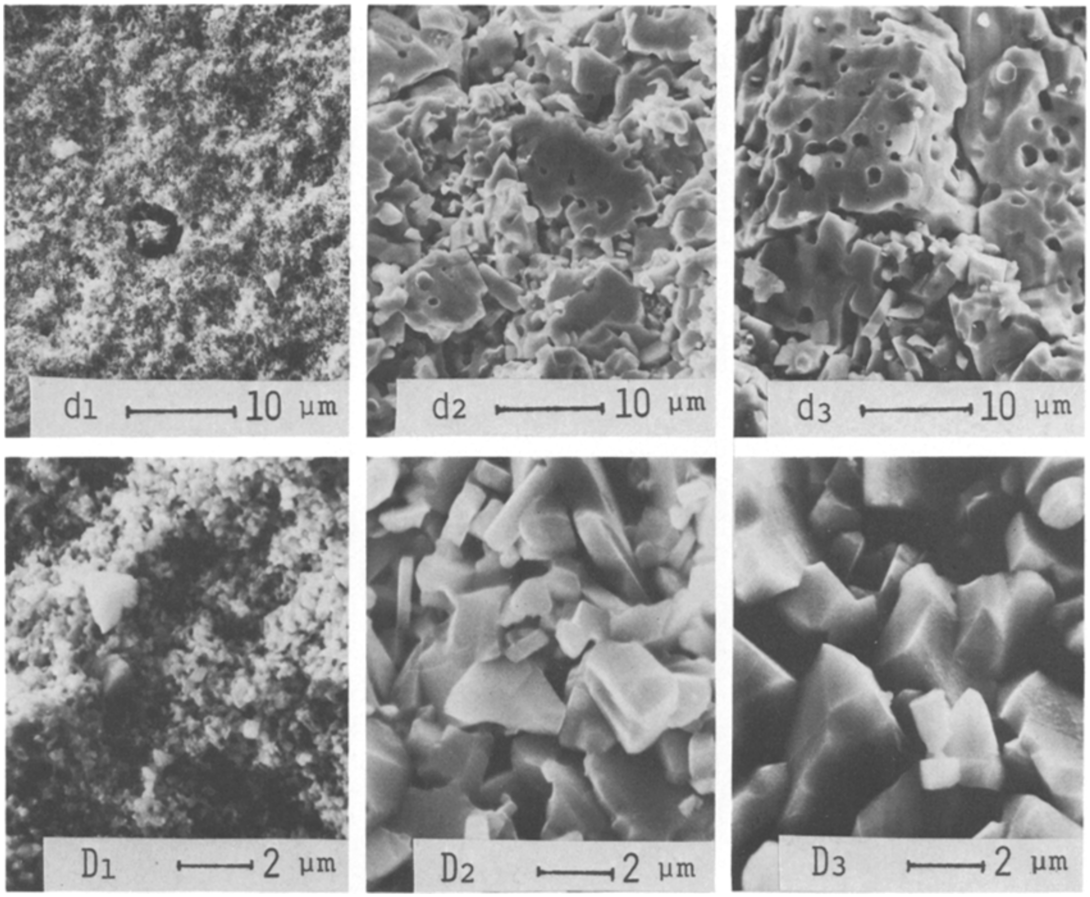

Figure 5 SEM photographs of fracture surfaces of D–WC sintered at 1500° C in hydrogen. Sintering time – d_1, D_1: 0.25 h; d_2, D_2: 0.5 h; d_3, D_3: 4 h.

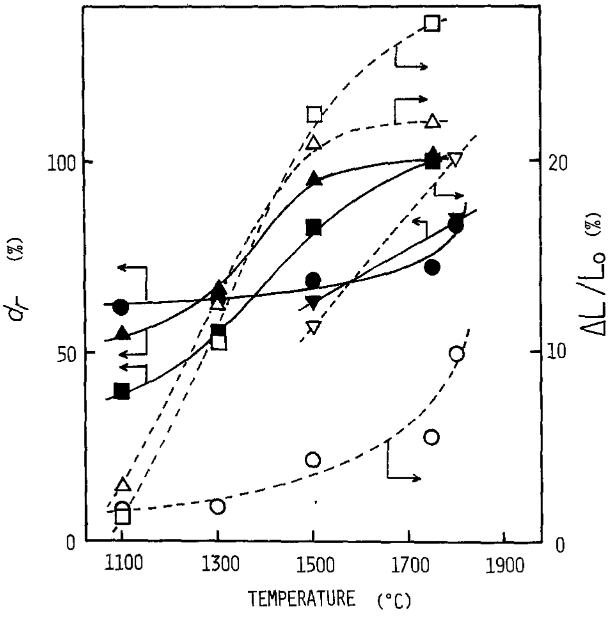

Figure 6 Effects of temperature on the sintering of WC powders in vacuum (heating: 0.5 h). The symbols are the same as in Fig. 2.

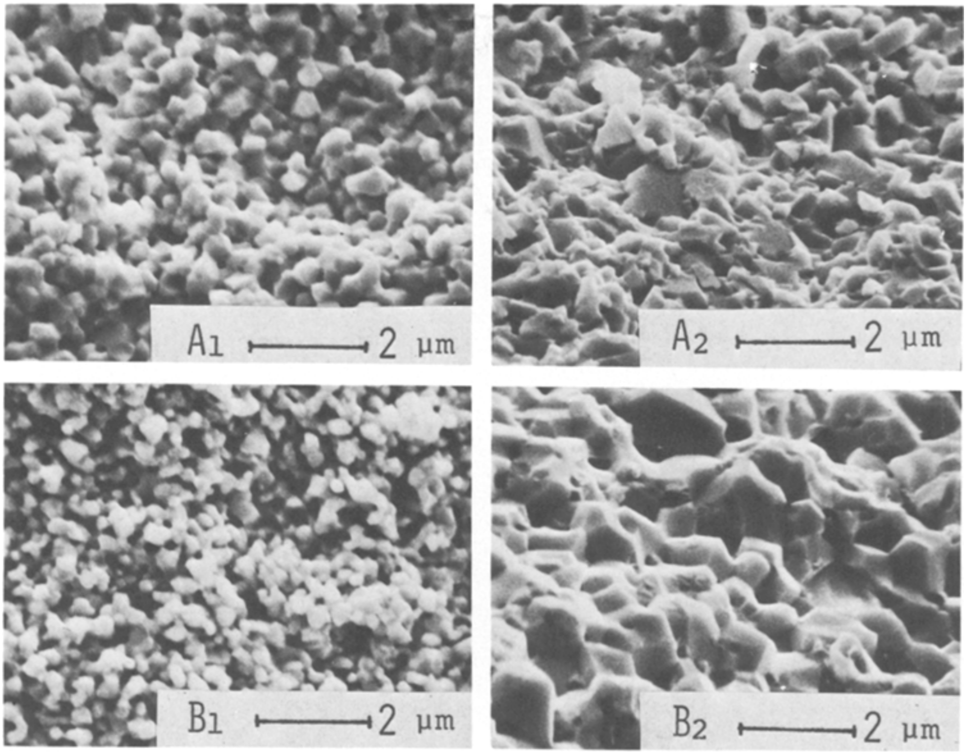

Figure 7 SEM photographs of fracture surfaces of A–WC and B–WC sintered for 0.5 h in vacuum. Sample (sintering temp.) – A_1: A–WC (1500° C); A_2: A–WC (1750° C); B_1: B–WC (1500° C); B_2: B–WC (1750° C).

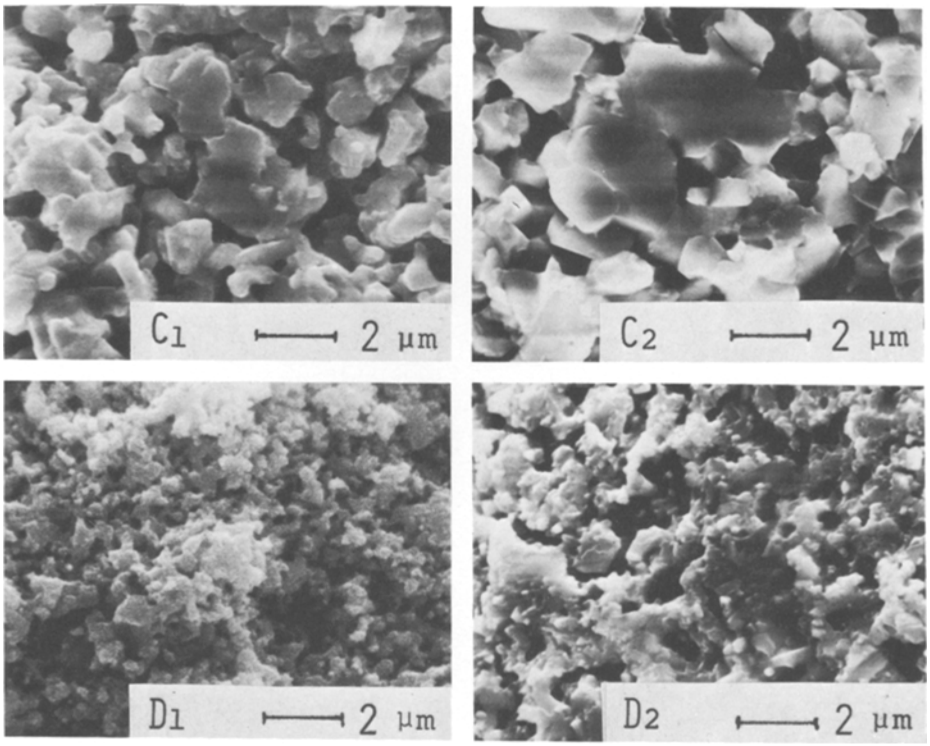

Figure 8 SEM photographs of fracture surfaces of C–WC and D–WC sintered for 0.5 h in vacuum. Sample (sintering temp.) – C_1: C–WC (1500° C); C_2: C–WC (1800° C); D_1: D–WC (1500° C); D_2: D–WC (1800° C).

TABLE III Foreign phases appearing in WC sintering (heating for 0.5 h)

Sample	Atmosphere	Sintering temperature (° C)				
		1100	1300	1500	1750	1800
A–WC	Hydrogen	n.d.	n.d.	n.d.	–	–
	Vacuum	n.d.	n.d.	n.d.	n.d.	–
B–WC	Hydrogen	n.d.	n.d.	n.d.	–	–
	Vacuum	W	n.d.	n.d.	n.d.	–
C–WC	Hydrogen	W	n.d.	n.d.	–	–
	Vacuum	W	W, W_2C	W_2C	W_2C	n.d.
D–WC	Hydrogen	W	n.d.	n.d.	–	–
	Vacuum	–	–	n.d.	–	n.d.

n.d.: not detected.

the dense microstructure is observed. However, the hardness values measured in the present work are lower than the values above 2500 kg mm^{-2} reported for sintered WC [3]. This suggests that the adhesion of WC grains is still incomplete under the present sintering conditions.

4. Discussion

4.1. Densification behaviour of WC powders

As seen in Fig. 3, the densification proceeds rapidly in the early stages of the sintering of WC powders. Suzuki *et al.* [4] and Saito *et al.* [5] reported that the particle rearrangement contributed significantly to the densification of the compact consisting of fine particles. The rapid densification of the compact of WC powders produced by the CVD method (A, B, D–WC) at the early stage may be mainly due to the particle rearrangement. The densities of the sintered A, B and D–WC increased gradually after the initial densification and changed little with time after 0.5 h when the grain growth became remarkable. This later densification seems to be caused by a sintering process consisting of adhesion of particles and grain growth. Thus, it could be mentioned that in the sintering of fine WC powders produced by the CVD method the densification of the compact proceeds mainly during a short time before the beginning of grain growth. The rapid densification of the compact of commercial WC powders (C–WC) with the large particle size and wide-size distribution may also be due to the particle rearrangement involving the fine particles contained in this sample.

4.2. Effects of particle size and atmosphere on sinterability

The sintering data of WC powders above 1500° C in hydrogen and vacuum were summarized in Table IV.

4.2.1. *Particle size effect*

In the sintering at 1500° C in hydrogen, the difference in sinterability among sample powders is too small to estimate the effect of the particle sizes. On the other hand, in the sintering in vacuum, the difference in sinterability among samples is significant. The densities of the sintered A and

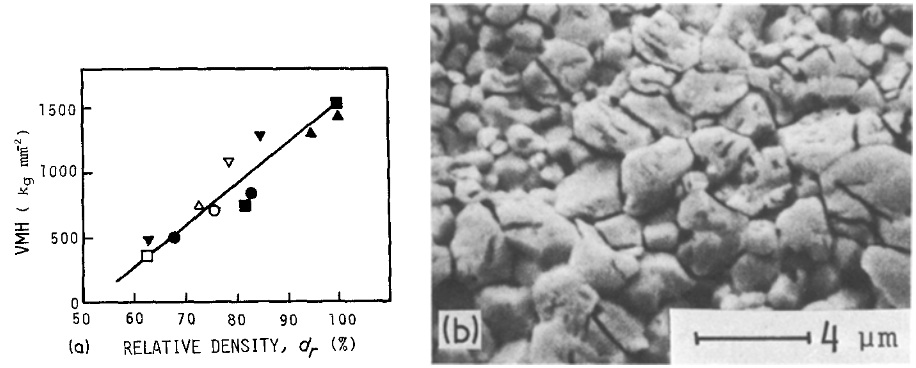

Figure 9 (a) Variation of Vickers micro-hardness (VMH) with relative density of WC sintered at 1500 to 1800° C for 0.5 h (open symbols: sintered in hydrogen; closed symbols: sintered in vacuum) and (b) SEM photograph of the etched section of B–WC sintered with the relative density of 100%. Load for the hardness measurement: 500 g. △, ▲: A–WC; □, ■: B–WC; ○, ●: C–WC; ▽, ▼ : D–WC.

TABLE IV Sintering data of WC powders above 1500° C in hydrogen and in vacuum (heating for 0.5 h)

Sample	Temp. (° C)	In hydrogen				In vacuum			
		$\Delta L/L_0$ (%)	d_r (%)	P_0 (%)	P_c (%)	$\Delta L/L_0$ (%)	d_r (%)	P_0 (%)	P_c (%)
A–WC	1500	13	73	27	0	21	95	5	0
	1750	–	–	–	–	22	100	0	0
B–WC	1500	17	63	36	1	22	82	10	8
	1750	–	–	–	–	27	100	0	0
C–WC	1500	8	78	22	0	4	69	31	0
	1750	–	–	–	–	6	72	27	1
	1800	–	–	–	–	10	83	15	2
D–WC	1500	14	79	14	7	11	63	36	1
	1800	–	–	–	–	20	85	15	0

$\Delta L/L_0$: linear shrinkage; d_r: relative density;
P_0, P_c: porosities (open pore and closed pore, respectively).

B–WC were higher in vacuum than in hydrogen and those of the sintered C and D–WC were lower in vacuum than in hydrogen. At 1500 to 1800° C in vacuum, the sinterabilities of WC powders decrease in the order of A–WC > B–WC > C–WC ≃ D–WC. The order of sinterability among A, B and C–WC agrees with predictions based on the order of particle size (A < B < C). However, the low sinterability of D–WC in vacuum cannot be explained by the particle size effect alone, since this sample D–WC was as fine as A–WC. As seen in Fig. 5, it is noted that the grain growth was more vigorous in D–WC than in A–WC in sintering in hydrogen, although both sintered bodies had a similar density to each other. The reason for the difference in sintering behaviour between A and D–WC may be the difference in chemical composition, i.e. D–WC contains foreign phases, W and W_2C, and has a high oxygen content. Furthermore, it should also be noted that the free carbon content of C–WC, which showed a low sinterability in vacuum, is less than those of A and B–WC. These facts suggest that the sinterabilities of WC powders are influenced significantly by their chemical compositions and sintering atmospheres as well as the particle sizes.

4.2.2. Atmospheric effect

The atmospheric effect on the sinterability of WC powders is estimated to be related closely to the chemical compositions of the original powders, especially the behaviour of a surface oxide layer and free carbon in the heating process. With respect to behaviour, the present authors have confirmed that the reduction of WO_3 powders to W starts at about 400° C in hydrogen, that the carburization of W powders with methane begins at about 800° C, that methane at a pressure of 10^{-3} atm is present in the atmosphere of the sintering in hydrogen (1100 to 1500° C)* and that WO_3 vaporizes above 1200° C in vacuum. The reduction and subsequent carburization of WO_3 with carbon are known to start at about 1000° C [6].

From these facts and the results in Table III, the behaviour of the surface oxide layer and free carbon of WC powders may be summarized as follows

In H_2,

$$WO_n + H_2 \longrightarrow W + H_2O \qquad (> \sim 400°\,C) \qquad (1)$$

$$W \xrightarrow{CH_4} W_2C,\ WC \qquad (> \sim 800°\,C) \qquad (2a)$$

$$W \xrightarrow{C_{free}} W_2C,\ WC \qquad (> \sim 1000°\,C) \qquad (2b)$$

In vacuum,

$$\left.\begin{array}{ll} WO_n + C_{free} \longrightarrow W + CO & (3) \\ W \xrightarrow{C_{free}} W_2C,\ WC & (4) \end{array}\right\} (> \sim 1000°\,C)$$

$$WO_n + WC \longrightarrow W, W_2C + CO \qquad (5)$$

$$WO_n \longrightarrow WO_x \text{ (vapour)} \qquad (> \sim 1200°\,C) \qquad (6)$$

---

*Methane is formed by the reaction between graphite and hydrogen.

On the basis of these results, the effect of atmosphere on the sinterability of WC powders is accounted for as follows. In the sintering of A and B–WC with much free carbon, the free carbon is considered to retard the sintering of WC particles. The higher sinterabilities of A and B–WC in vacuum compared with in hydrogen may be due to the fact that more free carbon is removed in vacuum than in hydrogen by reaction with the surface oxide layer. The reason for the lower sinterability of C–WC with a low free carbon content in vacuum compared with in hydrogen may be because the surface W_2C layer produced by the reaction of the oxide layer with the WC phase inhibits the sintering. This is supported by the fact that the density of the C–WC sintered in vacuum increased abruptly at about 1800° C whereas the W_2C phase disappeared. The sintering of D–WC with a high oxygen content resulted in a greater weight loss of compact in vacuum than in hydrogen (weight loss: 7% in hydrogen, 12% in vacuum), indicating that some tungsten was vaporized as oxide in vacuum. The lower sinterability of D–WC in vacuum compared with in hydrogen is estimated to be caused by the vaporization of surface oxide layer which may loosen the contact of particles.

5. Conclusion

The sintering behaviour of fine WC powders produced by a CVD method (particle size $< 0.3\,\mu$m) and commercial WC powders (particle size $\sim 1\,\mu$m) was investigated in hydrogen (1100 to 1500° C) and in vacuum (1100 to 1800° C). The following results were obtained.

(1) Fine WC powders have a high sinterability and give a sintered body with relative density of 100% by sintering at a low temperature such as 1750° C. WC powders with larger particle sizes show a high sinterability when the particle size distributions are wide. The densification of the compact of WC powders occurs rapidly at an early stage of sintering before the beginning of grain growth.

(2) The atmospheric and particle size effects are significant in the sintering of WC powders. The selection of atmosphere based on the amounts of surface oxygen and free carbon is important in obtaining a high density.

References

1. J. HOJO, T. OKU and A. KATO, *J. Less-Common Met.* **59** (1978) 85.
2. L. E. TOTH, "Transition Metal Carbides and Nitrides". In "Refractory Materials", Vol. 7, edited by J. L. Margrave (Academic Press, New York, 1971) p. 7.
3. K. KUDAKA, H. KONNO and T. MATOBA, *Nippon Kinzoku Gakkaishi* **31** (1967) 177.
4. H. SUZUKI and T. HATTORI, *Yogyo Kyokai shi* **77** (1969) 193.
5. S. SAITO, T. KONNO and A. SAWAOKA, *Japan. J. Appl. Phys.* **11** (1972) 628.
6. Y. HORIGUCHI, T. MATOBA and Y. ISHIMARU, *Denki Kagaku* **29** (1961) 773.

Received 24 September 1979 and accepted 15 February 1980.